IEEE Access
Multidisciplinary | Rapid Review | Open Access Journal

Received 6 September 2023, accepted 13 September 2023, date of publication 19 September 2023,
date of current version 27 September 2023.

Digital Object Identifier 10.1109/ACCESS.2023.3317230

RESEARCH ARTICLE

A New Fractional Reduced-Order Model-Inspired System Identification Method for Dynamical Systems

JUAN J. GUDE[1], ANTONIO DI TEODORO[2], OSCAR CAMACHO[2], (Senior Member, IEEE), AND PABLO GARCÍA BRINGAS[3]

[1]Department of Computing, Electronics and Communication Technologies, Faculty of Engineering, University of Deusto, 48007 Bilbao, Spain
[2]Colegio de Ciencias e Ingenierías "El Politécnico", Universidad San Francisco de Quito (USFQ), Quito 170157, Ecuador
[3]Department of Mechanics, Design and Industrial Management, Faculty of Engineering, University of Deusto, 48007 Bilbao, Spain

Corresponding author: Juan J. Gude (jgude@deusto.es)

The work of Juan J. Gude and Pablo García Bringas was supported by the Basque Government through the BEREZ-IA Elkartek Project under Grant KK-2023/00012. The work of Antonio Di Teodoro and Oscar Camacho was supported by Universidad San Francisco de Quito through the Poli-Grants Program under Grant 17965.

ABSTRACT This paper presents a new method for identifying dynamical systems to get fractional-reduced-order models based on the process reaction curve. This proposal uses information collected from the process. It can be applied to processes with an S-shaped step response that can be considered with fractional behavior and a fractional order range of $\alpha \in [0.5, 1.0]$. The proposed approach combines obtaining the fractional order of the model using asymptotic properties of the Mittag-Leffler function with time-based parameter estimation by considering two arbitrary points on the process reaction curve. The improvement in terms of accuracy of the identified FFOPDT model is obtained due to a more accurate estimation of α parameter. This method is characterized by its effectiveness and simplicity of implementation, which are key aspects when applying at an industrial level. Several examples are used to illustrate the effectiveness and simplicity of the proposed method compared to other well-established methods and other approaches based on the process reaction curve. Finally, it is also implemented on microprocessor-based hardware to demonstrate the applicability of the proposed method to identify the fractional model of a thermal process.

INDEX TERMS Fractional-order systems, process identification, fractional first-order plus dead-time model.

I. INTRODUCTION

To design and tune the controller of a feedback control loop, data about the dynamic behavior of the controlled process is required. This information is usually obtained from a reduced-order mathematical model [1].

From the perspective of the controller, the controlled process is composed of the process itself, including the final control element and the measuring instrument. In this context, the considered controlled process model provides the dynamics between the controller and the measurement instrument output signals. When considering this model, a balance must be sought between, on the one hand, simplicity in the estimation and use of such model and, on the other hand, the reliable information it must provide to estimate the impact of the control system on the behavior of the output variable of the controlled process at the operating point; see [2]. The information provided by the model typically includes the gain, the apparent dead-time, and the time constant(s) of the controlled process.

Despite all the progress achieved in process control during the last decades, the proportional-integral-derivative (PID) algorithm is certainly still the most extensive option encountered in industrial control applications and has become an important standard for the industrial and academic community, see [3]. The most common process models used for

The associate editor coordinating the review of this manuscript and approving it for publication was Norbert Herencsar.

the purpose of tuning this algorithm are first-order, second-order, and double-pole plus dead-time (FOPDT, SOPDT, and DPPDT). Since these models cannot characterize the process dynamics accurately in some cases, the controlled process needs to be identified with more accurate models to improve control loop performance. This has been suggested before in the technical literature, e.g., in [4], where it is already stated that more accurate process models are required to derive optimal PID tuning rules for lag-dominated processes.

One type of approach with a wide variety of identification procedures in the technical literature is one based on an open-loop test for integer-order models; see, for example, the identification procedures described in [5], [6], [7], and [8]. These identification methods require very limited information about the controlled process, making them very popular and appropriate for use in industry. More precisely, among the procedures based on open-loop step response, some references describing identification algorithms fitting different representative points on the process reaction curve can be highlighted, see [9], [10], and [11]. Generally, these identification methods are based on fitting two or three points on the reaction curve, considering FOPDT, SOPDT, and DPPDT models. In this context, methods using two and three points can be distinguished in the literature. In the first group, the following methods [11], [12], [13], [14] are prominent, while the methods [15], [16], [17] are considered in the second group. Note that the identification method considered in [11] is used as a two-point method for FOPDT and DPPDT models and a three-point method for SOPDT models.

Over recent decades, new computational techniques and fractional-order calculus have enabled a significant academic and industrial effort focused mainly on transitioning from classical controllers and models to those described by non-integer differential equations.

The main advantages of fractional derivatives are flexibility and non-locality. Since these derivatives are of fractional order, real data can be approximated with more flexibility with these operators than with classical ones. In addition, they also take into account non-locality, something that the classical derivatives cannot do. Therefore, they are more suitable for cases with memory (non-locality in time) and global interactions (non-locality in space). Regarding the transition from classical to fractional-order operators, the interested reader is referred to [18], which provides a list of proposals for non-integer order operators and derivatives, the classification of the current formulations for these operators, and a discussion of criteria for classifying fractional operators.

The progressive adoption of fractional calculus in industrial applications is motivated, on the one hand, by its apparent benefit in the field of modeling [19], [20], [21], and [22], which has been proven at the industrial level, and, on the other hand, by the clear advantages of fractional-order PID controllers over integer-order ones [23], [24], [25], [26]. Consequently, fractional-order dynamic models and controllers are increasingly present in industrial applications; see, e.g., [27] and [28].

In the context of methods for identifying fractional-order models based on the reaction curve, there is an emerging range of methods in the literature. Certainly, the most widely encountered approach in industrial practice is the one based on nonlinear optimization; see, e.g., [29], [30], [31], and [32]. They are generally performed by minimizing the error between the process reaction curve and the step response of the fractional-order model.

The identification procedures based on the process reaction curve described below are characterized as analytical techniques, their main feature being the simplicity of implementation. In [33], some strategies for estimating FFOPDT model parameters using data from the step response have been proposed. These strategies combine graphical estimation and numerical computation. The same author has proposed integral-based estimation methods, characterized by their robustness in the presence of measurement noise, in [34] and [35].

Recently, there has been renewed interest in extending classical three-point identification procedures for fractional-order processes. In this regard, Gude and García Bringas presented a general identification method for an FFOPDT model based on the process reaction curve in [36]. This identification method can be applied to any process that exhibits an S-shaped step response. The process information is taken from an open-loop step-test experiment by fitting three arbitrary points on the process reaction curve (x_1-x_2-x_3%). It has also been shown that the accuracy of the identified fractional-order model is sensitive to the location of the representative points on the reaction curve, and rules of thumb in selecting such a set of points are provided, see [36].

In [37], a simplification of the general identification procedure is proposed, considering that the three points are symmetrically located on the process reaction curve (x-50-(100 − x)%). In this way, the identification procedure is further simplified.

More recently, the influence of moving the central point x_2 on the process reaction curve while maintaining the symmetry of the extreme points (x_1 and x_3) with respect to the center of the total range has been studied in [38]. In this work, results with fractional-order models verify that the accuracy of the estimated model is sensitive to the position of the central point within the symmetrical set of points on the process reaction curve, and it has been discussed how a more accurately identified model can be determined.

These analytical techniques are characterized by requiring less computational effort and being simple to implement compared to optimization-based methods. Reference [39] presents the conceptualization of an efficient and practical control hardware architecture oriented toward implementing integer- and fractional-order identification and control algorithms. The applicability and effectiveness of the proposed control hardware architecture have been demonstrated by implementing the identification algorithms proposed in [36] and [37] in different hardware technologies.

TABLE 1. Summary of techniques for obtaining reduced-order models based on the process reaction curve.

Technique type	Model	Main characteristics	Ref.
two-point method three-point method	FOPDT DPPDT SOPDT	In this work, Alfaro presents an analytical general identification procedure for first- and second-order plus delay models, which uses two or three points on the process reaction curve. The characteristic points for FOPDT and DPPDT models are (25-75%), while the set of points used for SOPDT models is (25-50-75%).	[11]
two-point method	FOPDT	An analytical two-point method is proposed in this paper, which consists of a simple method to estimate the parameters of the FOPDT model considering two points (35-85%) on the process reaction curve.	[12]
two-point method	FOPDT	In this paper, the two-point method proposed by Smith consists of a simple method to estimate the parameters of the FOPDT model considering two points (28.3-63.2%) on the process reaction curve. In this case, the location of the points on the process reaction curve is related to the parameter T of the FOPDT model.	[13]
two-point method	FOPDT DPPDT	The analytical approach proposed by Miluse et al. in this paper identifies FOPDT or DPPDT models from an S-shaped step response of the process considering the set of points (33-70%).	[14]
three-point method	SOPDT	This paper presents an analytical identification method for SOPDT models considering three points, (2-70-90%) or (5-70-90%), on the process reaction curve. Analytical expressions for overdamped and underdamped responses are distinguished.	[15]
three-point method	SOPDT	In this paper, the three-point method proposed by Stark consists on a simple method for estimating SOPDT model parameters considering three points (15-45-75%) on the process reaction curve.	[16]
three-point method	SOPDT	This paper presents a simple method for estimating SOPDT model parameters considering three points (14-55-91%) on the process reaction curve.	[17]
optimization-based	FFOPDT	FFOPDT model identification method proposed by Malek is based on unconstrained nonlinear identification that minimizes the error signal between the fractional-order model step response and the process reaction curve.	[29]
optimization-based	FFOPDT	In this work, Ahmed proposes an integral equation approach for simultaneous estimation of model parameters and time delay from a single step data test, assuming that the fractional order is known.	[30]
optimization-based	FFOPDT	Guevara et al. present an FFOPDT model identification algorithm that applies an optimization procedure minimizing the integral of absolute error between the model step response and the process reaction curve. The fractional order range is $0.0 \leq \alpha \leq 2.0$, which includes overdamped and underdamped responses.	[31]
optimization-based	FFOPDT	Alagoz et al. present different approaches using two fundamental numerical solution methods of fractional calculus for identification of FFOPDT models. In this study, the step responses of an FFOPDT model are numerically calculated according to Mittag-leffler and Grünwald-Letnikov definitions. Particle Swarm Optimization algorithm is used to perform data fitting. The objective function to be minimized is the mean squared error.	[32]
integral-based	FFOPDT	This reference can be considered as a pioneering work in the identification of the FFOPDT model, which is used to characterize the dynamic response of those processes having S-shaped step responses. Three different approaches are proposed to estimate the parameters of the considered fractional-order model by making use of the step response data. It combines numerical computation and graphical estimation. The range of the identified fractional order is $0.0 \leq \alpha \leq 1.0$.	[33]
integral-based	FFOPDT	In this paper, an integral- based estimation method is proposed to identify an FFOPDT model. Its main feature is the robustness against the presence of measurement noise. The range of the identified fractional order is $0.0 \leq \alpha \leq 1.0$. This method can be considered as an extension of the existing classical area methods.	[34]
integral-based	FFOPDT	This paper deals with integral-based methods to estimate the order and parameters of simple fractional-order models from the extracted noisy step response data of a process. The range of the identified fractional order is $0.0 \leq \alpha \leq 1.0$.	[35]
three-point method	FFOPDT	This identification method for FFOPDT models proposed by Gude and García Bringas is based on fitting three arbitrary points (x_1-x_2-x_3%) on the process reaction curve. This analytical method is applied to processes characterized by an S-shaped step response and the range of the identified fractional order is $0.5 \leq \alpha \leq 1.0$.	[36]
three-point method	FFOPDT	This analytical fractional model identification method proposed by Gude and García Bringas is based on fitting three symmetrical points (x-50-$(100-x)$%) on the process reaction curve. This method is applied to processes characterized by an S-shaped step response and the range of the identified fractional order is $0.5 \leq \alpha \leq 1.0$.	[37]
three-point method	FFOPDT	This fractional model identification method proposed by Gude and García Bringas is based on fitting three symmetrical points (x-x_2-$(100-x)$%) on the process reaction curve, moving the central point x_2 while maintaining the symmetry of the extreme points $x_1 = x\%$ and $x_3 = (100-x)\%$. This analytical identification method is applied to processes characterized by an S-shaped step response and the range of the identified fractional order is $0.5 \leq \alpha \leq 1.0$.	[38]

For the reader's convenience, Table 1 summarizes the main characteristics of the different integer- and fractional-order model identification methods that are based on the process reaction curve and are cited above. The information contained in this table includes the reference of the identification method, the type of technique, the reduced-order model used, and the main characteristics of the method.

According to all the previously considered, obtaining a simple-structure fractional-order model for a process is of significant importance and very helpful for designing integer- or fractional-order control systems, particularly those of PID type.

This paper presents a new method for identifying fractional-order models based on the information collected from the process reaction curve. This method is applied to processes exhibiting fractional behavior, as explained in [40], with an S-shaped step response and a range of fractional order $\alpha \in [0.5, 1.0]$. The approach used combines obtaining the fractional order of the model using the asymptotic property of the Mittag-Leffler function in conjunction with the estimation of the time-based parameters $\{T, L\}$ by considering two

arbitrary points on the process reaction curve. Several examples will be used to illustrate the simplicity and effectiveness of the proposed procedure compared to other well-established methods and approaches based on the process reaction curve. Finally, it will also be implemented on microprocessor-based hardware in order to demonstrate the applicability of the proposed method for identifying the FFOPDT model of a thermal-based process.

The following is the structure of this paper. Section II presents some theoretical and preliminary background. In Section III, a new identification method for FFOPDT models is proposed based on information collected from the process reaction curve. The results of some numerical simulations and experimental tests are shown in Section IV to verify the efficiency and applicability of the proposed procedure in comparison with other well-recognized methods in the technical literature. Next, future works and research lines are described in Section V. Finally, Section VI concludes this paper.

II. PRELIMINARIES AND THEORETICAL BACKGROUND

This section briefly discusses some basic definitions and concepts of fractional-order calculus. These kinds of fundamental ideas about fractional calculus appear in several books, for instance, in [41], [42], and [43].

Fractional calculus is a generalization of the traditional calculus of real numbers to the case of non-integer orders. It was first developed by Gottfried Leibniz in the 17th century, but it did not gain widespread attention until the 20th century. Fractional calculus has applications in various fields, including physics, chemistry, engineering, and biology.

This section is divided into the following parts: The first part introduces the Riemann-Liouville and Caputo derivatives and their connection. In the second part, the behavior of the fractional order is considered in $\alpha \in (0, 1)$. The third part deals with the Mittag-Leffler function and its properties. Then, the Grünwald-Letnikov derivative, used for numerical computation, is defined. Finally, fractional-order models are discussed in the context of this work.

A. THE RIEMANN–LIOUVILLE AND THE CAPUTO FRACTIONAL DERIVATIVE

The Riemann-Liouville and Caputo derivatives are used to model and solve various problems. For example, they can be used to model the behavior of systems with memory or that exhibit non-local behavior. They can also solve differential equations that are not solvable with traditional integer-order calculus.

We introduce both derivatives and their connections to have a complete idea of how they work and what we can expect of each one.

The first step is to define the Riemann–Liouville fractional integral of order $\alpha > 0$ by (see [41], [44], [45], [46]).

$$\left(I^{\alpha}_{a^+}h\right)(x) = \frac{1}{\Gamma(\alpha)}\int_a^x \frac{h(t)}{(x-t)^{1-\alpha}}\,dt, \quad x > a. \tag{1}$$

We denote by $I^{\alpha}_{a^+}(L_1)$ the class of functions h, represented by the fractional integral of a summable function, that is, $h = I^{\alpha}_{a^+}\varphi$, where $\varphi \in L_1(a, b)$, $\alpha \in \mathbb{R}$ and Γ is the gamma function. A description of this class of functions is given in [44] and [46].

The Riemann–Liouville and the Caputo fractional derivatives are defined (see [44], [46], [47], [48]):

Definition 1: Let $\alpha \geq 0$ and $m = [\alpha]$, where $[\alpha]$ denotes the integer part of α. The Caputo fractional derivative ${}_c\mathcal{D}^{\alpha}_{a^+}$ is given by [41], [44], and [46]:

$$\left({}_cD^{\alpha}_{a^+}f\right)(t) := I^{m-\alpha}_{a^+}\left(\frac{d}{dx}\right)^m f, \tag{2}$$

whenever $\left(\frac{d}{dx}\right)^m f \in L_1[a, b]$.

Definition 2: Let $\alpha \geq 0$ and $m = [\alpha]$, the Riemann–Liouville fractional derivative ${}_{RL}\mathcal{D}^{\alpha}_{a^+}$ is given by [41], [44], and [46]:

$${}_{RL}\mathcal{D}^{\alpha}_{a^+} = \left(\frac{d}{dx}\right)^m \left(I^{m-\alpha}_{a^+}\right)f, \tag{3}$$

with $f \in L_1[a, b]$

Connection between both derivatives:

Lemma 1: Let $\alpha \geq 0$ and $m = [\alpha] + 1$. Suppose that f is such that ${}_cD^{\alpha}_{a^+}$ and ${}_{RL}D^{\alpha}_{a^+}$ exists. Then

$${}_cD^{\alpha}_{a^+}f = {}_{RL}\,D^{\alpha}_{a^+}f - \sum_{k=0}^{m-1}\frac{(x-a)^{k-\alpha}}{\Gamma(k-\alpha+1)}\left(\frac{d}{dx}\right)^k f(a),$$

Proof of Lemma 1: See [44], [46], and [49].

As a consequence of the previous Lemma, we can have the following result:

Lemma 2: Let $\alpha \geq 0$ and $m = [\alpha]$. Assume that f is such that both ${}_cD^{\alpha}_{a^+}$ and ${}_{RL}D^{\alpha}_{a^+}$ exist. Then ${}_cD^{\alpha}_{a^+}f = {}_{RL}\,D^{\alpha}_{a^+}f$ if and only if $\left(\frac{d}{dx}\right)^k f(a) = 0$ for $k = 0, \ldots, m-1$.

Proof of Lemma 2: Follow by direct calculation from the previous Lemma.

For example, when $0 < \alpha < 1$, then (3) takes the form

$${}_{RL}\mathcal{D}^{\alpha}_{a^+}h(x) = \frac{d}{dx}\frac{1}{\Gamma(1-\alpha)}\int_a^x \frac{h(t)}{(x-t)^{\alpha}}dt.$$

B. BEHAVIOR OF THE FRACTIONAL PARAMETER α

In this subsection, we will rely on polynomials to understand how the derivatives work and the behavior of fractional operators changes as we approach the fractional parameter α to the edges of the intervals where they are defined. Through this discussion, we aim to clarify why we can perceive fractional calculus as a generalization of classical calculus, despite relinquishing locality.

Let $\alpha \in (0, 1)$. Then we consider the real Riemann-Liouville fractional polynomials defined as (see [47], [48]):

$$\Phi^{\alpha,m} := \frac{(x-a)^{(m+1)\alpha-1}}{\Gamma(\alpha)\,\Gamma((m+1)\alpha)}, m \in \mathbb{N}_0. \tag{4}$$

where $\frac{1}{\Gamma(\alpha)\Gamma((m+1)\alpha)}$ can be interpreted as a non-constant deformation factor of the classical operators. Such fractional polynomials have the following fractional properties:

Proposition 1: Let $\alpha \in (0,1)$, $a > 0$, $k \in \mathbb{N}$ and $m \in \mathbb{N}_0$, then

i $\quad {}_{I}D_{a^+}^{k-\alpha}\Phi^{\alpha,m} = \frac{(x-a)^{m\alpha+k-1}}{\Gamma(\alpha)\Gamma(m\alpha+k)}$,

ii $\quad {}_{RL}D_{a^+}^{\alpha}\Phi^{\alpha,m} = \begin{cases} 0, & m=0, \\ \Phi^{\alpha,m-1}, & m \in \mathbb{N}, \end{cases}$.

Proof of Proposition 1: Both result from direct calculation and definition.

This proposition is well defined for all fractional operators and fractional polynomials defined when $\alpha \in (0,1)$. We now explore its behavior at the boundaries 0^+ and 1^-. For that matter, we state the following result on the fractional polynomials.

Proposition 2: Let $\alpha \in (0,1)$, $a > 0$ and $m \in \mathbb{N}_0$ then

1. $\lim_{\alpha\to 1^-} \Phi^{\alpha,m} = \frac{(x-a)^m}{m!}$
2. $\lim_{\alpha\to 0^+} \Phi^{\alpha,m} = 0$

Proof of Proposition 2: We will prove the first result using the definition of $\Phi^{\alpha,m}$ in (4):

$$\lim_{\alpha\to 1^-} \Phi^{\alpha,m} = \lim_{\alpha\to 1^-} \left[\frac{(x-a)^{(m+1)\alpha-1}}{\Gamma(\alpha)\,\Gamma((m+1)\alpha)} \right].$$

We know that the gamma function $\Gamma(z)$ is continuous for $z > 0$, also ([44], [46]),

$$\lim_{\alpha\to 1^-} \Gamma((m+1)\alpha) = \Gamma(m+1) = m!, m \in \mathbb{N}_0,$$

On the other hand, the continuity of $(x-a)^z$ with respect to $z \in \mathbb{R}$, tells us that

$$\lim_{\alpha\to 1^-} (x-a)^{(m+1)\alpha-1} = (x-a)^m, m \in \mathbb{N}_0.$$

Finally, since $\lim_{\alpha\to 1^-} \Gamma(\alpha) = 1$, the result follows. For the second statement, we follow a similar reasoning.

We now state similar results for the fractional derivative and integral of our fractional polynomials.

Proposition 3: Let $\alpha \in (0,1)$, $a > 0$, $k \in \mathbb{N}$ and $m \in \mathbb{N}_0$ then

1. $\lim_{\alpha\to 1^-} \left[{}_{I}D_{a^+}^{k-\alpha}\Phi^{\alpha,m} \right] = \frac{(x-a)^{m+k-1}}{(m+k-1)!}$,
2. $\lim_{\alpha\to 1^-} \left[{}_{RL}D_{a^+}^{\alpha}\Phi^{\alpha,m} \right] = \begin{cases} 0, & m=0 \\ \frac{(x-a)^{m-1}}{(m-1)!}, & m \neq 0 \end{cases}$,
3. $\lim_{\alpha\to 0^+} \left[{}_{I}D_{a^+}^{k-\alpha}\Phi^{\alpha,m} \right] = 0$,
4. $\lim_{\alpha\to 0^+} \left[{}_{RL}D_{a^+}^{\alpha}\Phi^{\alpha,m} \right] = 0$.

Proof of Proposition 3: Results 1 and 3 follow by continuity of all terms in both right-hand side expressions below:

$$\lim_{\alpha\to 1^-} \left[{}_{I}D_{a^+}^{k-\alpha}\Phi^{\alpha,m} \right] = \lim_{\alpha\to 1^-} \frac{(x-a)^{m\alpha+k-1}}{\Gamma(\alpha)\,\Gamma(m\alpha+k)},$$

$$\lim_{\alpha\to 0^+} \left[{}_{I}D_{a^+}^{k-\alpha}\Phi^{\alpha,m} \right] = \lim_{\alpha\to 0^+} \alpha \frac{(x-a)^{m\alpha+k-1}}{\Gamma(\alpha+1)\,\Gamma(m\alpha+k)}.$$

Results 2 and 4 follow as a direct consequence of propositions 1 and 2 by evaluating

$$\lim_{\alpha\to 1^-} \left[{}_{RL}D_{a^+}^{\alpha}\Phi^{\alpha,m} \right] = \lim_{\alpha\to 1^-} \begin{cases} 0, & m=0, \\ \Phi^{\alpha,m-1}, & m \in \mathbb{N}, \end{cases},$$

$$\lim_{\alpha\to 0^+} \left[{}_{RL}D_{a^+}^{\alpha}\Phi^{\alpha,m} \right] = \lim_{\alpha\to 0^+} \begin{cases} 0, & m=0, \\ \Phi^{\alpha,m-1}, & m \in \mathbb{N}, \end{cases}.$$

Remark 1: If $k = 1$, by proposition 1, we have that $\lim_{\alpha\to 1^-} \left[{}_{I}D_{a^+}^{1-\alpha}\Phi^{\alpha,m} \right] = \frac{(x-a)^m}{m!} = I^0 \left[\lim_{\alpha\to 1^-} \Phi^{\alpha,m} \right]$. Where I^0 denotes the identity operator such that $I^0[f(x)] = f(x)$.

Remark 2: Interestingly enough, if $k = 2$, we have that $\lim_{\alpha\to 1^-} \left[{}_{I}D_{a^+}^{2-\alpha}\Phi^{\alpha,m} \right] = \frac{(x-a)^{m+1}}{(m+1)!} = J \left[\lim_{\alpha\to 1^-} \Phi^{\alpha,m} \right]$, where J denotes the classical integral operator $J[f(x)] = \int_a^x f(t)\,dt$.

Remark 3: If $k = 1$, we have that $\lim_{\alpha\to 1^-} \left[{}_{RL}D_{a^+}^{\alpha}\Phi^{\alpha,m} \right] = \frac{(x-a)^{m-1}}{(m-1)!} = \frac{d}{dx} \left[\lim_{\alpha\to 1^-} \Phi^{\alpha,m} \right]$, where $\frac{d}{dx}$ denotes the classical differential operator.

In other words from the previous remark, if α approaches 1 from the left, the fractional integral operator ${}_{I}D_{a^+}^{k-\alpha}$ becomes the identity when $k = 1$ and the classical integral operator when $k = 2$; furthermore, the fractional differential operator ${}_{RL}D_{a^+}^{\alpha}$ becomes the classical first-order one. Also, all fractional polynomials $\Phi^{\alpha,m}$ become classical ones (with natural or null power m).

Moreover, propositions 2 and 3 show that ${}_{I}D_{a^+}^{1-\alpha}$ becomes the classical integral operator and ${}_{RL}D_{a^+}^{\alpha}$ becomes the identity one as α approaches to 0 from the right. Although it seems trivial, this result complements the previous remarks because it is well-known that real fractional operators converge to the classical ones as α goes to the frontiers of $(0,1)$.

From an operator's point of view (see [44], [46], [50]), the real differential property $\lim_{\alpha\to 1^-} {}_{RL}D_{x_l^+}^{\alpha} = \partial_{x_l}$ is supported by definitions of the Riemann–Liouville fractional integral and differential operator.

C. THE TWO-PARAMETER MITTAG-LEFFLER FUNCTION AND ITS PROPERTIES

Definition 3: The two-parameter function of the Mittag-Leffler type, which plays a very important role in fractional calculus [51], [52], for an arbitrary value $z \in \mathbb{C}$ can be defined as:

$$E_{\alpha,\beta}(z) = \sum_{r=0}^{\infty} \frac{z^r}{\Gamma(\alpha r + \beta)}, \tag{5}$$

where $\alpha \in \mathbb{R}^+$, $\beta \in \mathbb{C}$, and $\Gamma(\cdot)$ is the Gamma function, [41], [44].

This function is uniformly convergent over $\mathbb{C}$ with the following properties:

Let $\alpha, \beta \geq 0$

(i) If $\beta = 1$. The function coincides with the classical one-parameter Mittag-Leffler function, i.e.,

$E_{\alpha,1} = E_\alpha$, which for an arbitrary value z is defined as:

$$E_\alpha(z) = \sum_{r=0}^{\infty} \frac{z^r}{\Gamma(\alpha r + 1)}, \tag{6}$$

(ii) If $\alpha = 1$ and $\beta = 1$. The function coincides with the exponential.

$$E_{1,1}(z) = E_1(z) = exp(z) \tag{7}$$

(iii) If $\alpha = 1$ and $\beta = \frac{1}{2}$

$$E_{\frac{1}{2},1}(z) = E_{\frac{1}{2}}(z) = exp(z^2)\ \text{erfc}(-z) \tag{8}$$

Theorem 1: Asymptotic behavior of the Mittag-Leffler function. Let $\alpha \in (0, 2)$ and $\beta \in \mathbb{C}$, let $\mu \in \mathbb{R}$ arbitrary, such that $\frac{\pi\alpha}{2} < \mu < min\{\pi, \pi\alpha\}$. Then, for an arbitrary integer $p \geq 1$, the following asymptotic expansion holds:

$$E_{\alpha,\beta}(z) = \frac{1}{\alpha} z^{(1-\beta)/\alpha} exp(z^{1/\alpha}) - \sum_{r=1}^{p} \frac{z^{-r}}{\Gamma(\beta - \alpha r)} + O(z^{-1-p}), \tag{9}$$

as $|z| \to \infty$ and $|argz| \leq \mu$. The proof can be found directly on page 32, Theorem 1.3 of the book [41].

And changing the location of the complex plane results in the following result:

Theorem 2: Asymptotic behavior of the Mittag-Leffler function. Let $\alpha \in (0, 2)$ and $\beta \in \mathbb{C}$, let $\mu \in \mathbb{R}$, such that $\frac{\pi\alpha}{2} < \mu < min\{\pi, \pi\alpha\}$. Then, for an arbitrary integer $p \geq 1$, the following asymptotic expansion holds:

$$E_{\alpha,\beta}(z) = -\sum_{r=1}^{p} \frac{z^{-r}}{\Gamma(\beta - \alpha r)} + O(z^{-1-p}), \tag{10}$$

as $z \to \infty$ and $\mu \leq |argz| \leq \pi$.

The proof can be found directly on page 33, Theorem 1.4 of the book [41].

Remark 4: The results remain valid for any sub interval A of $(0, 2)$.

D. GRÜNWALD-LETNIKOV DERIVATIVE

In this work, we will use the Grünwald-Letnikov derivative, which is advantageous to the numerical computation given that it is defined in a discrete way. And can be obtained as a limiting case of the Riemann-Liouville derivative. More precisely, we have:

$${}_{RL}D_a^\alpha f(x) = \lim_{h \to 0} \frac{1}{h^\alpha} \sum_{k=0}^{\infty} (-1)^k \binom{\alpha}{k} \frac{f(x - kh)}{\Gamma(n - \alpha)(x - kh - a)^{n-\alpha}} \tag{11}$$

where $n - 1 < \alpha < n$ and h is a step size which converge to (see [44], [45], [46], [49]).

E. PROCESS MODELS

In the context of this paper, where process control problems are dealt with, the following general form of a fractional-order transfer function representation of a process model is used:

$$P(s) = \frac{\sum_{i=0}^{m} b_i s^{\beta_i}}{\sum_{i=0}^{n} a_i s^{\alpha_i}} e^{-Ls}, \tag{12}$$

where $a_i, b_i \in \mathbb{R}$, $\alpha_i, \beta_i \in \mathbb{R}^+$, and $L \in \mathbb{R}^+$. It it is common to take $\beta_0 = \alpha_0 = 0$ so that the static gain of the system is given by $K = b_0/a_0$.

The particular case where ($b_m = b_{m-1} = \ldots = b_1 = 0$; $a_n = a_{n-1} = \ldots = a_2 = 0$; $a_1 = T$; $a_0 = 1$; $b_0 = K$; $\beta_0 = 0$; $\alpha_1 = \alpha$; $\alpha_0 = 0$) leads to the following fractional-order differential equation:

$$T \cdot D^\alpha y(t) + y(t) = K \cdot u(t - L), \tag{13}$$

where K is the process gain, $T > 0$ is the time constant, $L \geq 0$ is the apparent deadtime, and α is the fractional order of the model. The initial conditions are generally taken as zero to obtain the FFOPDT transfer function model:

$$P(s) = \frac{K \cdot e^{-Ls}}{1 + Ts^\alpha}, \tag{14}$$

Figure 1 shows the step responses of the FFOPDT model for increasing values of α, with $\alpha \in [0.2, 1.8]$. The dashed line represents the step response of the system for $\alpha = 1$, which corresponds to the standard FOPDT model.

The following set of parameters:

$$\theta_P = \{K, T, L, \alpha\}, \tag{15}$$

represents the FFOPDT model parameters, which will be identified in this paper using information taken from the process reaction curve.

III. MODEL IDENTIFICATION METHOD

In this section, the expressions for estimating the parameters of the FFOPDT model are developed. The approach considered ingeniously combines techniques used in other identification methods but which have never been used together. On the one hand, the estimation of parameter α is obtained by exploiting the asymptotic behavior of the Mittag-Leffler function, as proposed, e.g., in [33]. On the other hand, the model parameters T and L are estimated using two arbitrary points on the process reaction curve, as discussed in [36].

Figure 2 illustrates a step signal $u(t)$ with amplitude Δu as input, and a signal $y_\alpha(t)$ with an amplitude variation of Δy as system response. FFOPDT model (14) response to a Δu step input change is:

$$y_\alpha(t) = \begin{cases} 0, & 0 \leq t < L \\ K\left[1 - E_{\alpha,1}[-\frac{1}{T}(t - L)^\alpha]\right]\Delta u, & t \geq L \end{cases} \tag{16}$$

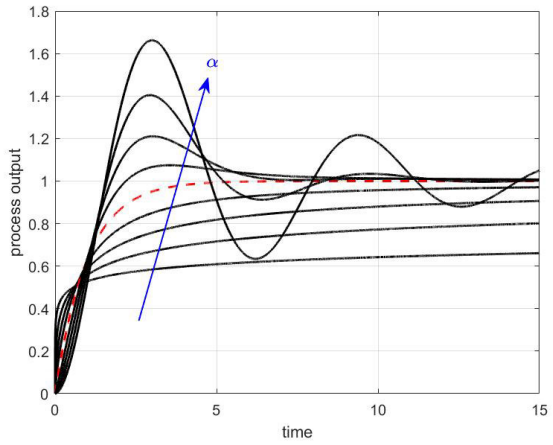

FIGURE 1. FFOPDT model step responses for different values of $\alpha \in [0.2, 1.8]$. The response is either overdamped or underdamped depending on the value of α. The case for FOPDT models, $\alpha = 1$, is depicted in red dashed line.

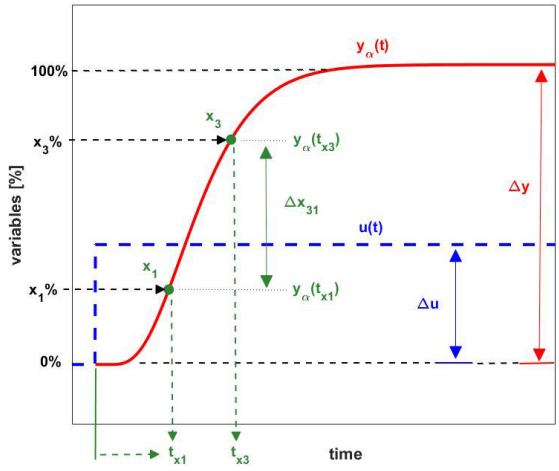

FIGURE 2. Step input signal $u(t)$, S-shaped step response signal $y_\alpha(t)$, and the corresponding representative points x_1 and x_3 on the process reaction curve.

where $E_{\alpha,\beta}$ is the two-parameter Mittag-Leffler function, which was previously defined in (5).

Remark 5: The expressions of $y_\alpha(t)$ for the boundary values of α are: $\lim_{\alpha\to 1^-} y_\alpha(t) = K\big[1 - exp\big[-\frac{1}{T}(t-L)\big]\big]\Delta u$, and $\lim_{\alpha\to 0^+} y_\alpha(t) = K\big[1 - \sum_{r=0}^{\infty}\big(-\frac{1}{T}\big)^r\big]\Delta u$

In this context, t_x represents the time required for the process output to reach $x\%$ of the process output total change, which corresponds to the point $y_\alpha(t_x)$ on the process reaction curve.

Normalizing the process output $y_\alpha(t)$ with respect to the process output total change $\Delta y = K \cdot \Delta u$ and substituting the time variable t for the shifted and normalized time $\tau = \frac{1}{T}(t-L)^\alpha$, eq. (16) is reduced to the following expression:

$$\tilde{y}_\alpha(\tau) = 1 - E_{\alpha,1}(-\tau), \qquad \tau \geq 0 \tag{17}$$

In this context, τ_x is the normalized time required for the normalized process output to reach $x\%$ of the normalized process output total change, which corresponds to the point $\tilde{y}_\alpha(\tau_x)$ on that curve. Figure 3 illustrates the normalized process output $\tilde{y}_\alpha(t/T_{ar})$ for different values of $\alpha \in [0.5, 1.0]$, where $T_{ar} = L + T^{1/\alpha}$ is the average residence time.

In the following subsections, the parameters of the FFOPDT model, $\theta_P = \{K, T, L, \alpha\}$, will be estimated. The estimation of K is performed conventionally, as for integer-order models. The parameter α is obtained from the asymptotic behavior of the system step response $y_\alpha(t)$. Finally, the time-based model parameters, $\{T, L\}$, are estimated by considering two arbitrary points on the process reaction curve.

A. ESTIMATION OF K

The gain K for model (14) can be obtained from the process reaction curve based on the following expression:

$$K = \frac{\Delta y}{\Delta u}, \tag{18}$$

where Δy is the process output total change to the step input change Δu, as shown in Fig. 2. In this respect, the estimation method for the static gain K is the same as for integer-order models.

B. ESTIMATION OF α

In this work, parameter α can be estimated directly from the process reaction curve. In this regard, the asymptotic behavior of the Mittag-Leffler function is exploited.

Considering the step response of the FFOPDT model in eq. (16) and the asymptotic behavior of the Mittag-Leffler function, as expressed in eq. (10), the asymptotic behavior of $\bar{y}_\alpha(t)$ can be well approximated by the function:

$$\bar{y}_\alpha(t) \simeq K - \eta t^{-\alpha}, \tag{19}$$

where $\bar{y}_\alpha(t)$ is the unit step response of the system, i.e., $\bar{y}_\alpha(t) = \frac{y_\alpha(t)}{\Delta u}$ and η is a finite constant value. From (19), parameter α can be estimated as:

$$\alpha = -\lim_{t\to\infty} \frac{log[K - \bar{y}_\alpha(t)]}{log(t)}, \tag{20}$$

In the above expression, the value of the parameter α can be determined by considering the negative slope of $log[K - \bar{y}_\alpha(t)]$ with respect to $log(t)$ for large values of t.

C. ESTIMATION OF T AND L

If $\tilde{y}_\alpha(\tau_x)$ is a specific output normalized value –being between 0 and 1, or 0% and 100% of the process output total change– the normalized time τ_x can be obtained using (17). Then, the time t_x required for the process output (16) to reach such point is:

$$t_x = L + (\tau_x T)^{1/\alpha}, \tag{21}$$

Remark 6: It is important to note that $\alpha \in (0, 1]$ for the expression (21) to make sense.

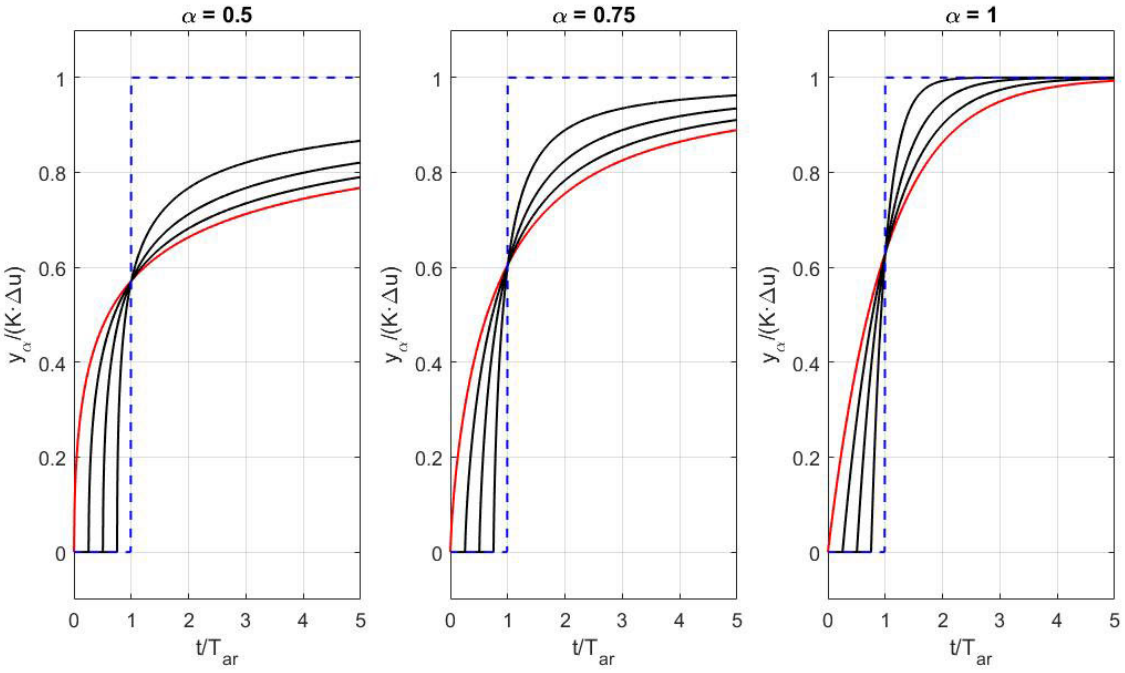

FIGURE 3. Normalized step responses $y_\alpha/(K \cdot \Delta u)$ of the FFOPDT model for different values of the normalized dead-time $\tau_\alpha = L/(L + T^{1/\alpha})$. In the figure, the normalized dead-times used are $\tau_\alpha = 0$ (red), 0.25, 0.5, 0.75, and 1 (blue). Note that the cases $\alpha = 0.5$, 0.75, and 1 have been considered and that the time is normalized with respect to the average residence time $T_{ar} = L + T^{1/\alpha}$.

The time-based parameters $\{T, L\}$ can be solved by considering two points, $\{y_\alpha(t_{x1}), t_{x1}\}$ and $\{y_\alpha(t_{x3}), t_{x3}\}$, on the reaction curve. Then, the following set of equations is defined:

$$\begin{cases} t_{x1} = L + (\tau_{x1} T)^{1/\alpha} \\ t_{x3} = L + (\tau_{x3} T)^{1/\alpha} \end{cases} \tag{22}$$

The corresponding two equivalent normalized points considered for estimating parameters $\{T, L\}$ are $\{\tilde{y}_\alpha(\tau_{x1}), \tau_{x1}\}$ and $\{\tilde{y}_\alpha(\tau_{x3}), \tau_{x3}\}$, respectively.

Combining both expressions, the model parameters T and L can be obtained as functions of the times $\{t_{x1}, t_{x3}\}$ and the normalized times $\{\tau_{x1}, \tau_{x3}\}$:

$$T = a^\alpha (t_{x3} - t_{x1})^\alpha, \tag{23}$$

where

$$a = \frac{1}{(\tau_{x3}^{1/\alpha} - \tau_{x1}^{1/\alpha})}, \tag{24}$$

and

$$L = t_{x3} - \tau_{x3}^{1/\alpha} T^{1/\alpha}. \tag{25}$$

Note that functions $f_2(\alpha)$ and $f_3(\alpha)$ can be defined from (23) and (25), which depend on α and the normalized times τ_{x1} and τ_{x3}, and τ_{x3}, respectively.

$$f_2(\alpha) = a^\alpha, \tag{26}$$

$$f_3(\alpha) = \tau_{x3}^{1/\alpha}, \tag{27}$$

Functions f_2 and f_3 are determined from the data sets $\{\alpha, a^\alpha\}$ and $\left\{\alpha, \tau_{x3}^{1/\alpha}\right\}$ for $0.5 \leq \alpha \leq 1.0$ and are generally expressed by rational functions resulting from least-squares curve fitting for the selected set of points (x_1-x_3%).

In conclusion, the expressions for determining the time-based model parameters, $\{T, L\}$, using the times required for the response to reach two arbitrary points x_1 and x_3 on the process reaction curve, t_{x1} and t_{x3}, are as follows:

$$\begin{cases} T = f_2(\alpha)(t_{x3} - t_{x1})^\alpha \\ L = t_{x3} - f_3(\alpha) T^{1/\alpha} \end{cases} \tag{28}$$

In (28), $\alpha > 0$ is considered and $T > 0$ is fulfilled in a natural way, since $\tau_{x1} < \tau_{x3}$ and $t_{x1} < t_{x3}$. Another condition that must be fulfilled in order to meet $L \geq 0$ is the following:

$$t_{x3} \geq (\tau_{x3} T)^{(1/\alpha)}. \tag{29}$$

D. ALGORITHM

To facilitate software implementation, the identification method proposed in this paper is developed below in the form of an algorithm. The algorithm can be divided into two parts: an initialization part, where the rational expressions for $f_2(\alpha)$ and $f_3(\alpha)$ are determined as functions of α and the selected points x_1 and x_3, and another part that includes the main algorithm. In this method, the variation of the input signal Δu and the process output Δy, and the times required to reach x_1% (t_{x1}) and x_3% (t_{x3}) of the process output total change on the reaction curve must be collected in order to estimate the FFOPDT model parameters $\theta_P = \{K, T, L, \alpha\}$.

Algorithm 1 FFOPDT Model Identification Method Using the Asymptotic Property of the Mittag-Leffler Function and Two Points on the Process Reaction Curve

Input: times $\{t_{x1}, t_{x3}\}$, Δy, and Δu collected from the process reaction curve

Output: FFOPDT model parameters $\theta_P = \{K, T, L, \alpha\}$

Initialization:

1: Selection of points x_1 and x_3 on the process reaction curve

2: Determination of normalized times τ_{x1} and τ_{x3} using eq. (17)

3: Determination of data sets $\{\alpha, a^\alpha\}$ and $\left\{\alpha, \tau_{x3}^{1/\alpha}\right\}$ in the range $0.5 \leq \alpha \leq 1.0$ for obtaining $f_2(\alpha)$ and $f_3(\alpha)$ functions according to (26) and (27)

4: Calculation of rational expressions for functions $f_2(\alpha)$ and $f_3(\alpha)$ by using least-squares curve fitting

Main Algorithm:

5: Calculate the process gain K using (18)

6: Estimate the value of α using expression (20)

7: Calculate the value of functions $f_2(\alpha)$ and $f_3(\alpha)$ for the estimated value of α using rational expressions obtained in step 4

8: Determine the value of T using equation (23)

9: Determine the value of L using equation (25)

10: **return** θ_P

Note that all expressions used in the identification algorithm are analytical. This makes its implementation significantly simpler.

E. LIMITATIONS

The following are some observations and comments on the limitations of the identification method in industrial practice:

1) This work is restricted to identifying processes exhibiting fractional behavior, characterized by a monotonic S-shaped response and with an order in the range $0.50 \leq \alpha \leq 1.00$. Such processes with essentially monotonic step responses are prevalent in process control [2].
2) In an industrial environment, it is common for the feedback signal of the controlled process to include measurement noise that must be properly filtered for model identification and control purposes. Since the filter dynamics will be an integral part of the controlled process to be identified, measurement noise has not been considered in the proposed identification procedure.
3) It is widely known in the industrial context that processes present nonlinearities. The dynamic characteristics of the process change with the operating point of the control loop, which may vary due to a change in the setpoint or due to the effect of disturbances. Therefore, it must be considered that there is an implicit uncertainty in the nominal model. Since the main use of the identified fractional-order model is to design the control system, the usual approach is to consider the model uncertainty at the controller design stage; see, for example, [2] for integer-order controllers and [27] for fractional-order controllers. Thus, a certain degree of robustness of the designed control system against model uncertainties is guaranteed.

These two last aspects have been discussed in detail in the context of identification procedures based on the process reaction curve in [36].

TABLE 2. Parameters $\{p_i, q_i\}$ of the rational functions $f_2(\alpha)$ and $f_3(\alpha)$ for the set of points (10-90%).

$f_2(\alpha)$	$f_3(\alpha)$
$p_1 = -0.05698$	$p_1 = 4.518$
$p_2 = 0.1596$	$p_2 = -8.675$
–	$p_3 = 5.666$
$q_1 = -2.528$	$q_1 = -0.3471$
$q_2 = 1.753$	$q_2 = 0.003197$

IV. ILLUSTRATIVE EXAMPLES

The previous section has discussed the proposed procedure for identifying an FFOPDT model based on the process reaction curve.

Model parameters are obtained by selecting two arbitrary points (x_1-x_3%) on the reaction curve and exploiting the process response's asymptotic behavior. The latter is characteristic of the response for processes exhibiting fractional behavior.

In this section, the proposed FFOPDT model identification procedure has been tested for two fractional-order process models and a thermal process-based hardware-in-the-loop experimental setup.

Even being a general method valid for any set of points (x_1-x_3%) on the process reaction curve, without loss of generality, the set of points (10-90%), corresponding to $x_1 = 10\%$ and $x_3 = 90\%$ of the process output total change, will be used in this paper.

In this regard, the considered data sets $\{\alpha, f_2(\alpha)\}$ and $\{\alpha, f_3(\alpha)\}$ are determined for the set of points (10-90%) using the values of the corresponding normalized times $\{\tau_{10}, \tau_{90}\}$, for $0.50 \leq \alpha \leq 1.00$.

The following rational functions have been used for curve fitting of functions $f_2(\alpha)$ and $f_3(\alpha)$, respectively:

$$f_2(\alpha) = \frac{p_1\alpha + p_2}{\alpha^2 + q_1 + q_2}, \tag{30}$$

$$f_3(\alpha) = \frac{p_1\alpha^2 + p_2\alpha + p_3}{\alpha^2 + q_1 + q_2}, \tag{31}$$

Figure 4 shows data sets $\{\alpha, f_2(\alpha)\}$ and $\{\alpha, f_3(\alpha)\}$ and curves obtained by least-squares fitting using the Levenberg-Marquardt algorithm. The corresponding parameter values $\{p_i, q_i\}$ for functions $f_2(\alpha)$ and $f_2(\alpha)$ are shown in Table 2.

The numerical values of f_2 and f_3, which depend on the value of α that has been estimated, can be incorporated into

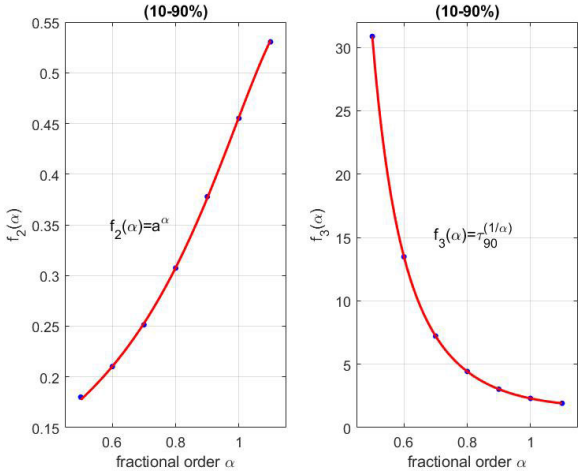

FIGURE 4. a) Data set $\{\alpha, f_2(\alpha)\}$ and function obtained by curve fitting for set of points (10-90%); b) Data set $\{\alpha, f_3(\alpha)\}$ and function obtained by curve fitting for set of points (10-90%).

eq. (28) in order to determine time-based parameters $\{T, L\}$. Note that the determination of the model parameters K and α is independent of the points x_1 and x_3 selected on the process reaction curve.

The selection of these values of x_1 and x_3 has been made taking into account that the accuracy of the identified model improves the larger the distance between x_1 and x_3, particularly in the interval $[x_1 - x_3]$. More specifically, the influence of the position of the representative symmetrical points on the accuracy of the identified model is treated in detail in [37].

Finally, the accuracy of the identified model needs to be evaluated. The mean squared error (MSE) is used as the time-domain fitting criterion to measure the performance of the identified model:

$$S(\theta) = \frac{1}{N_S}\sum_{k=1}^{N_S}[e(kT_S,\theta)]^2 = \frac{1}{N_S}\sum_{k=1}^{N_S}[y(kT_S) - y_m(kT_S,\theta)]^2, \quad (32)$$

where T_S is the sampling period, N_S is the number of samples collected, $N_S T_S$ is the time duration of the dynamic response, θ is the vector of process model parameters, and $e(kT_S, \theta)$ is the difference between the process reaction curve and the step response of the identified model, $y(kT_S)$ and $y_m(kT_S, \theta)$, respectively.

Remark 7: Note that the simulation results of Examples 1 and 2 have been implemented using MATLAB and the FOTF (Fractional Order Transfer Function) toolbox.

FOTF is a toolbox that extends many built-in MATLAB functions to deal with fractional-order systems and has been developed by Xue and collaborators [53]. Example 3 has been developed using LabVIEW, see [39]. In both MATLAB and LabVIEW, the numerical computation of the fractional-order models and step responses has been performed using the Grünwald-Letnikov definition for the fractional-order derivative. The sampling period is $T_S = 0.01$ s for Examples 1 and 2 and $T_S = 0.1$ s for Example 3. The number of samples N_S for each example is given in Tables 5, 9, and 13.

TABLE 3. Process information required for FFOPDT model identification of process P_1 using the proposed method.

Process $P_1(s)$ Proposed method (10-90%)
$\Delta u = 1.00$
$\Delta y = 3.00$
$t_{10} = 2.0290$ s
$t_{90} = 20.8030$ s

This section is organized as follows. First, two examples with higher-order fractional process models are used to compare the effectiveness of the proposed identification method with other well-known identification methods. Next, a thermal process-based hardware-in-the-loop experimental setup is used to verify the proposed identification method's applicability and test the identification algorithm's implementation on microprocessor-based industrial hardware. Finally, a discussion of the obtained results is presented.

A. EXAMPLE 1

In this example, a higher-order lag-dominated fractional-order process model is selected:

$$P_1(s) = \frac{K_1}{\prod_{i=1}^{3}(1 + T_i s^{\alpha_1})}, \quad (33)$$

where $K_1 = 3$, $T_1 = 1$ s, $T_2 = 2$ s, $T_3 = 3$ s, and $\alpha_1 = 0.88$.

This model has been initially proposed in [33] as an illustrative example and has also been used to verify the effectiveness of the method proposed by Gude and García Bringas in [36], which identifies FFOPDT model parameters using three arbitrary points, both symmetrical and asymmetrical, on the process reaction curve.

In this example, the FFOPDT model obtained using the proposed identification method is compared with those obtained using other well-known identification methods.

The step signal applied to the considered process P_1 as an open-loop test and the corresponding process reaction curve obtained for this fractional-order model are depicted in Fig. 5. Table 3 summarizes the process information required to identify the FFOPDT model with the proposed method considering the set of points (10-90%).

Figure 6 illustrates the step response of the estimated model using the proposed identification method and the corresponding process reaction curve.

Additionally, process (33) has also been approximated using several integer- and fractional-order models. More specifically, it has been approximated using an FFOPDT model obtained with the identification procedure described by Gude and García Bringas in [36] for the symmetrical (10-50-90%) and asymmetrical (10-55-90%) set of points,

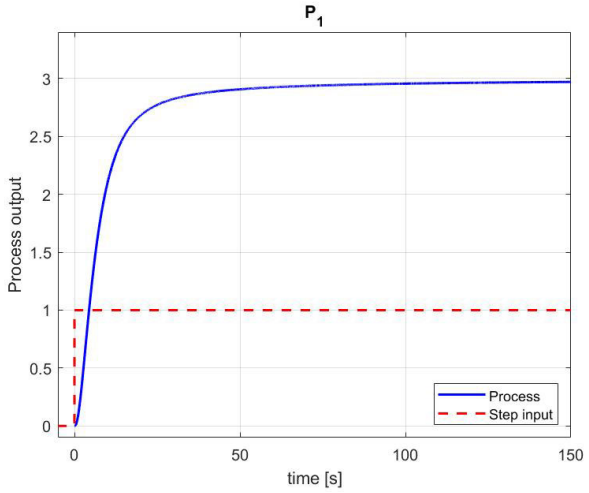

FIGURE 5. Process information required for the identification of the FFOPDT model: Step signal and reaction curve for process P_1.

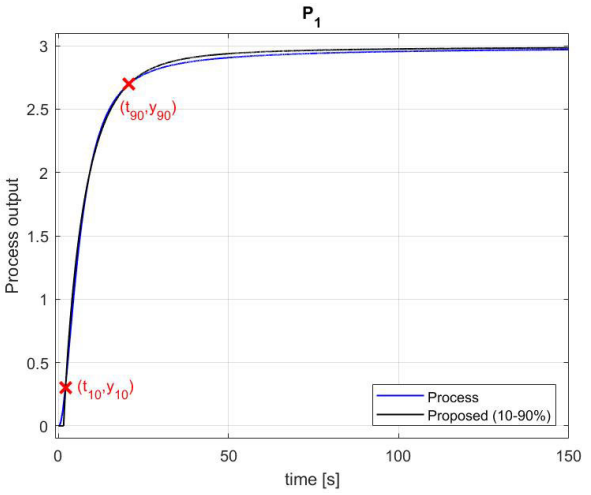

FIGURE 6. Process reaction curve for the considered process P_1 and FFOPDT model step response using the proposed identification procedure for (10-90%). Representative points $x_1 = 10\%$ and $x_3 = 90\%$ on the process reaction curve are also displayed. The figure shows that the step response of the FFOPDT model obtained with the proposed method accurately fits the process reaction curve.

TABLE 4. FFOPDT model parameters obtained for process P_1 with the different identification methods considered ($j = 1, \ldots, 5$) and optimal parameters obtained for an FOPDT model ($j = 6$).

j	Model parameters $\theta_{1,j}$			
1	$K_{1,1} = 3.00$	$T_{1,1} = 5.81$ s	$L_{1,1} = 1.51$ s	$\alpha_{1,1} = 0.920$
2	$K_{1,2} = 3.00$	$T_{1,2} = 6.64$ s	$L_{1,2} = 1.39$ s	$\alpha_{1,2} = 0.947$
3	$K_{1,3} = 3.00$	$T_{1,3} = 6.38$ s	$L_{1,3} = 1.43$ s	$\alpha_{1,3} = 0.939$
4	$K_{1,4} = 3.00$	$T_{1,4} = 6.30$ s	$L_{1,4} = 1.00$ s	$\alpha_{1,4} = 0.920$
5	$K_{1,5} = 3.00$	$T_{1,5} = 5.63$ s	$L_{1,5} = 1.88$ s	$\alpha_{1,5} = 0.926$
6	$K_{1,6} = 3.00$	$T_{1,6} = 8.74$ s	$L_{1,6} = 0.00$ s	–

the FFOPDT model obtained with the method followed by Tavakoli-Kakhki in [33], using an FFOPDT model determined with the optimization-based procedure described by Guevara et al. in [31], and using an optimal FOPDT model.

The model parameters $\theta_{1,j} = \{K_{1,j}, T_{1,j}, L_{1,j}, \alpha_{1,j}\}$ for $j = 1, \ldots, 6$, corresponding to the above methods, are shown in Table 4.

In order to evaluate the accuracy of the different identified models, the time-domain model performance index values $S(\theta_{1,j})$ for the models obtained with the considered identification methods ($j = 1, \ldots, 6$) applied to process P_1 are shown in Table 5. The values of the relative performance index $S_{1,j} = S(\theta_{1,1})/S(\theta_{1,j})$ for the models obtained using the different methods ($j = 1, \ldots, 6$) compared to the one for the proposed method ($j = 1$) are shown in Table 6 and illustrated in Fig. 7. This figure shows that the proposed method reduces by 37%, 25%, 40%, 29%, and 71%, the value of S to methods proposed by Gude for a symmetrical set of points (10-50-90%) and for an asymmetrical set of points (10-55-90%), by Tavakoli-Kakhki, by Guevara et al., and for optimal FOPDT model, respectively.

In summary, this example shows that the proposed method significantly improves the accuracy of the estimated FFOPDT model while maintaining the simplicity of the procedure compared to other well-known identification methods.

TABLE 5. Performance indexes obtained with the model obtained using the proposed method and the ones with several methods based on the process reaction curve for process P_1.

j	Method	Set of points	$S(\theta_{1,j})$
1	Proposed	(10-90%)	$8.14 \cdot 10^{-4}$
2	Symmetrical	(10-50-90%)	$1.29 \cdot 10^{-3}$
3	Asymmetrical	(10-55-90%)	$1.08 \cdot 10^{-3}$
4	Tavakoli-Kakhki	–	$1.36 \cdot 10^{-3}$
5	Guevara et al.	–	$1.14 \cdot 10^{-3}$
6	Optimal FOPDT	–	$2.80 \cdot 10^{-3}$
Number of samples: $N_S = 15,001$			

TABLE 6. Relative performance indexes obtained with different identification methods ($j = 1, \ldots, 6$) in comparison with the proposed method ($j = 1$) for process P_1. The improvement obtained by using the proposed method is also illustrated in this table.

j	Compared methods	$S_{1,j}$	Improvement
1	Proposed-Proposed	1.0000	–
2	Proposed-Symmetrical	0.6287	37%
3	Proposed-Asymmetrical	0.7551	25%
4	Proposed-Tavakoli-Kakhki	0.5982	40%
5	Proposed-Guevara	0.7138	29%
6	Proposed-Optimal FOPDT	0.2901	71%

B. EXAMPLE 2

In this example, the following higher-order lag-dominated fractional-order process model is selected:

$$P_2(s) = \frac{K_2}{(1 + T_2 s^{\alpha_2})^n}, \tag{34}$$

where $K_2 = 2$, $T_2 = 1$ s, $n = 5$, and $\alpha_2 = 0.85$.

This model has been proposed in [33] as an illustrative example and has also been used to verify the effectiveness of the methods proposed by Gude and García Bringas in [37], which identifies the FFOPDT model parameters using three symmetrical points on the process reaction curve, and

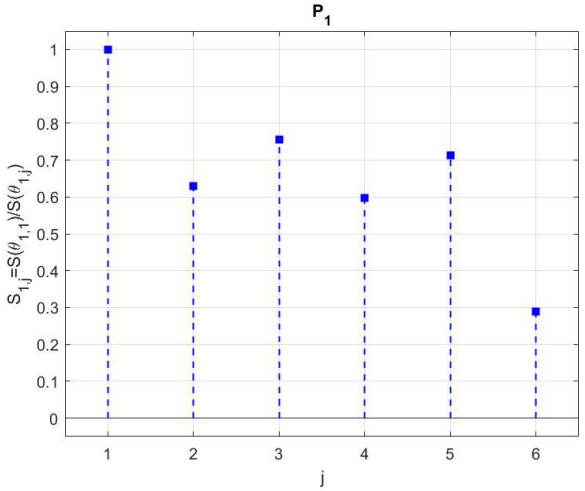

FIGURE 7. Relative performance index-based comparison between results obtained with different identification methods ($j = 1, \ldots, 6$) and the one obtained with proposed method ($j = 1$) for process P_1.

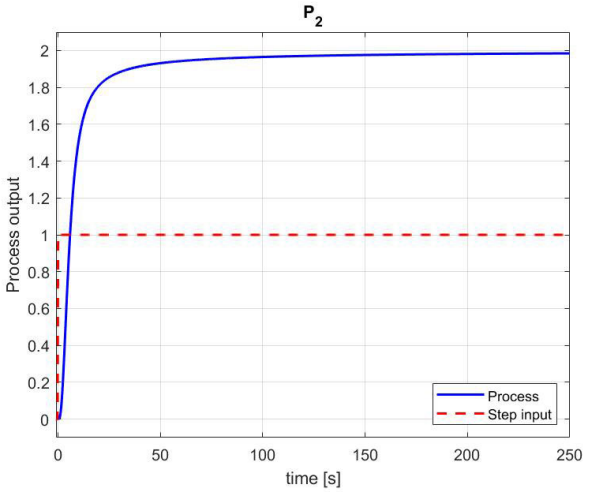

FIGURE 8. Process information required for the identification of the FFOPDT model: Step signal and reaction curve for process P_2.

TABLE 7. Process information required for FFOPDT model identification of process P_2 using the proposed method.

Process $P_2(s)$ Proposed method (10-90%)
$\Delta u = 1.00$
$\Delta y = 2.00$
$t_{10} = 2.3450$ s
$t_{90} = 19.2050$ s

in [38], where the accuracy of the identified FFOPDT model is improved by moving the central point x_2 on the process reaction curve. In this example, the FFOPDT model obtained using the proposed identification method is compared with those obtained with other well-recognized identification methods.

Figure 8 depicts the step-input signal of an open-loop test applied to process P_2 and the process reaction curve.

TABLE 8. FFOPDT model parameters obtained for process P_2 with the different identification methods considered ($j = 1, \ldots, 6$).

j	Model parameters $\theta_{2,j}$			
1	$K_{2,1} = 2.00$	$T_{2,1} = 4.44$ s	$L_{2,1} = 2.00$ s	$\alpha_{2,1} = 0.884$
2	$K_{2,2} = 2.00$	$T_{2,2} = 5.07$ s	$L_{2,2} = 1.89$ s	$\alpha_{2,2} = 0.912$
3	$K_{2,3} = 2.00$	$T_{2,3} = 4.34$ s	$L_{2,3} = 2.00$ s	$\alpha_{2,3} = 0.879$
4	$K_{2,4} = 2.00$	$T_{2,4} = 5.00$ s	$L_{2,4} = 1.50$ s	$\alpha_{2,4} = 0.850$
5	$K_{2,5} = 2.00$	$T_{2,5} = 5.00$ s	$L_{2,5} = 0.69$ s	$\alpha_{2,5} = 0.850$
6	$K_{2,6} = 2.00$	$T_{2,6} = 4.48$ s	$L_{2,6} = 1.50$ s	$\alpha_{2,6} = 0.850$

TABLE 9. Performance indexes obtained with the model obtained using the proposed method and the ones with several methods based on the process reaction curve for process P_2.

j	Method	Set of points	$S(\theta_{2,j})$
1	Proposed	(10-90%)	$2.91 \cdot 10^{-4}$
2	Symmetrical	(10-50-90%)	$4.49 \cdot 10^{-4}$
3	Asymmetrical	(10-65-90%)	$2.90 \cdot 10^{-4}$
4	Tavakoli-Kakhki 1	–	$1.10 \cdot 10^{-3}$
5	Tavakoli-Kakhki 2	–	$1.90 \cdot 10^{-3}$
6	Tavakoli-Kakhki 3	–	$6.56 \cdot 10^{-4}$
Number of samples: $N_S = 25,001$			

The process information required to identify the FFOPDT model with the proposed method considering the set of points (10-90%) is summarized in Table 7.

The step response of the proposed FFOPDT model is compared with the reaction curve in Fig. 9. Process P_2 has also been approximated using an FFOPDT model obtained with the identification procedure described by Gude and García Bringas [37] for the set of symmetrical points (10-50-90%), the model obtained with the identification procedure proposed by Gude [38] for the set of asymmetrical points (10-65-90%), and the models obtained by applying three strategies proposed by Tavakoli-Kakhki [33].

Table 8 shows the parameters of the FFOPDT model $\theta_{2,j} = \{K_{2,j}, T_{2,j}, L_{2,j}, \alpha_{2,j}\}$ for $j = 1, \ldots, 6$, corresponding to the above methods.

Table 9 shows the values of the time-domain model performance index $S(\theta_{2,j})$ for the models obtained with the considered identification methods ($j = 1, \ldots, 6$) applied to process P_2.

The values of the relative performance index $S_{2,j} = S(\theta_{2,1})/S(\theta_{2,j})$ for the models obtained using the different methods ($j = 1, \ldots, 6$) compared to the one for proposed method ($j = 1$) are shown in Table 10 and illustrated in Fig. 10.

This figure shows that the model obtained with the proposed method presents the same accuracy as the one obtained with the method proposed by Gude for the asymmetrical set of points (10-65-90%) and reduces by 35%, 74%, 85%, and 56% the value of S with respect to the models obtained with the method proposed by Gude for the symmetrical set of points (10-50-90%), and the ones obtained using the three strategies proposed by Tavakoli-Kakhki, respectively.

To conclude, this example also demonstrates that the proposed method provides a significant improvement in the accuracy of the estimated fractional-order model. Simplicity

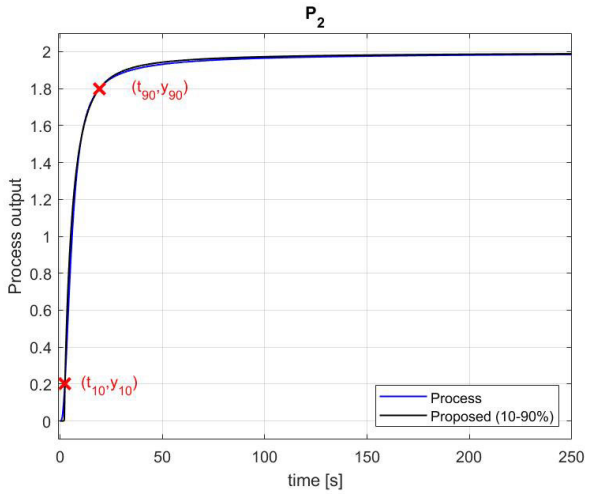

FIGURE 9. Process reaction curve for the considered process P_2 and FFOPDT model step response using the proposed identification procedure for (10-90%). Representative points $x_1 = 10\%$ and $x_3 = 90\%$ on the process reaction curve are also displayed. The figure shows that the step response of the FFOPDT model obtained with the proposed method accurately fits the process reaction curve.

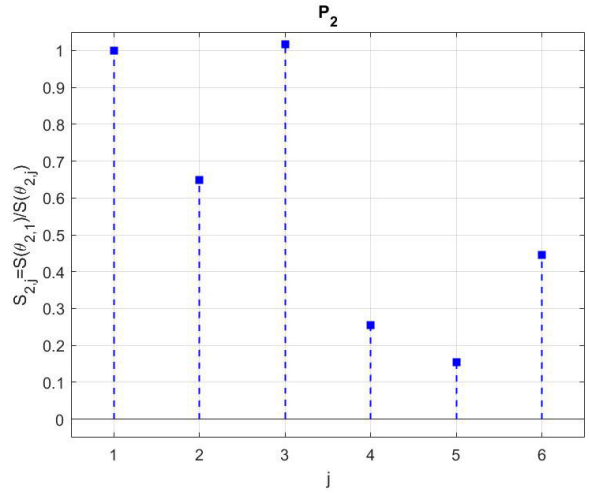

FIGURE 10. Relative performance index-based comparison between results obtained with different identification methods ($j = 1, \ldots, 6$) and the one obtained with proposed method ($j = 1$) for process P_2.

and effectiveness of the proposed procedure compared to other well-known identification methods are also remarkable.

C. EXAMPLE 3

This section uses a thermal process-based hardware-in-the-loop experimental setup that has recently been conceived and built and is used [39].

The controlled process in the apparatus consists of the thermodynamic temperature process in a 3D-printer extruder head, which is inside a methacrylate duct, and with an air fan installed in front of the hot end.

Figure 11 shows a picture of the experimental prototype detailing the different heat transfer forms in the extruder head.

TABLE 10. Relative performance indexes obtained with different identification methods ($j = 1, \ldots, 6$) in comparison with the proposed method ($j = 1$) for process P_2. The improvement obtained by using the proposed method is also illustrated in this table.

j	Compared methods	$S_{2,j}$	Improvement
1	Proposed-Proposed	1.0000	–
2	Proposed-Symmetrical	0.6481	35%
3	Proposed-Asymmetrical	1.0034	0%
4	Proposed-Tavakoli-Kakhki 1	0.2645	74%
5	Proposed-Tavakoli-Kakhki 2	0.1532	85%
6	Proposed-Tavakoli-Kakhki 3	0.4436	56%

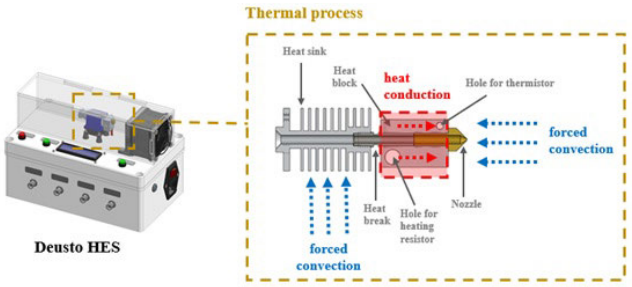

FIGURE 11. Picture of the experimental prototype and detail of the thermal-based process in the extruder head.

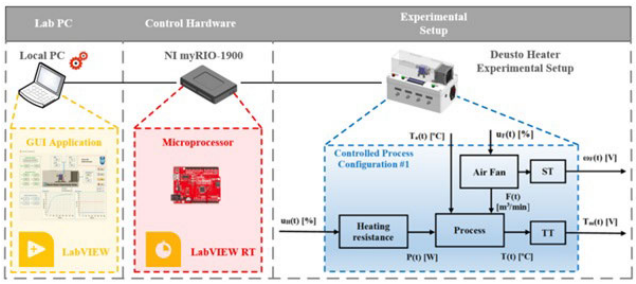

FIGURE 12. Scheme of the experimental setup, including the prototype configured with Controlled Process Configuration #1 and the microprocessor-based hardware architecture for implementation of fractional-order model identification algorithms. The local PC, where the graphical user interface is implemented, is also depicted in the figure.

The control hardware can control the air fan and the heating power of the resistance inside the extruder head. Thus, the controlled process can be configured to control the temperature in the heat block under different configurations. For this paper, configuration #1, which uses the heating resistor as the final control element while the air fan speed is kept constant, will be the selected configuration.

In this work, the control hardware architecture proposed in [54] is used for the implementation of the FFOPDT model identification algorithm proposed in the previous section.

For a more detailed description of this laboratory equipment, the conceptualization and the potential advantages of this hardware architecture over other available alternatives for the implementation of integer- and fractional-order model identification algorithms, the reader is referred to [39].

Figure 12 schematizes the experimental setup. It consists of the prototype, which shows the block diagram corresponding

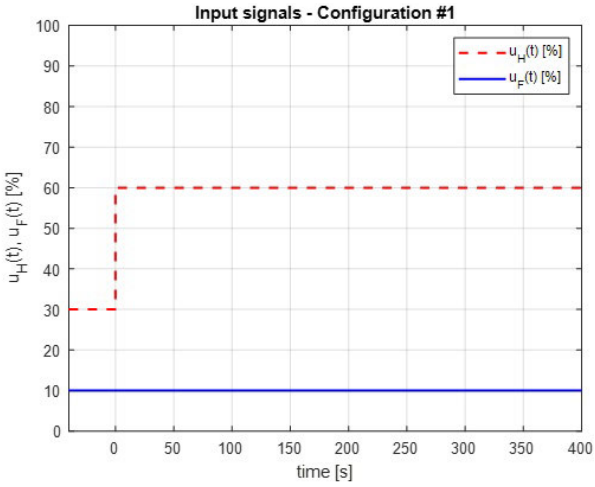

FIGURE 13. Input signals for experimental open-loop step test: control signal to the heating resistance $u_H(t)$ [%] and command signal to air fan $u_F(t)$ [%]. Experimental setup is configured with Controlled Process Configuration #1.

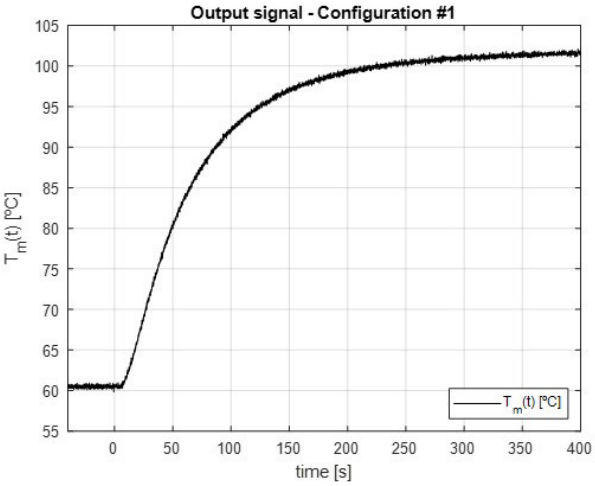

FIGURE 14. Output signal for open-loop step test: Process reaction curve $T_m(t)$ [^oC]. Experimental setup is configured with Controlled Process Configuration #1.

to the selected configuration of the controlled process, the hardware device, where the proposed identification algorithm is implemented, and the local PC, where the graphical user interface is displayed.

The experimental procedure to determine process data required to estimate an FFOPDT model consists of a typical step-input experimental test.

Initially, a step-input signal of magnitude $\Delta u_H = 30\%$ is applied to the heating element, while the command signal to the fan u_F is kept constant ($u_F = 10\%$), as illustrated in Fig. 13. The process reaction curve T_m at this operating point shows a variation of $\Delta T_m = 42^oC$ (from 60.5^oC to 102.5^oC), as shown in Fig. 14.

Table 11 shows the process information required to estimate K, T and L model parameters, while α parameter is estimated by using the process reaction curve $T_m(t)$.

TABLE 11. Process information required for FFOPDT model identification of the experimental controlled process using the proposed method with set of points (10-90%).

Experimental Setup Proposed method (10-90%)
$\Delta u = \Delta u_H = 30\%$
$\Delta y = \Delta T_m = 42^oC$
$t_{10} = 16.80$ s
$t_{90} = 174.50$ s

TABLE 12. FFOPDT model parameters obtained for the experimental controlled process using the proposed identification procedure with set of points (10-90%), and the ones obtained using the identification method proposed in [38] considering $x_1 = 10\%$ and $x_3 = 90\%$ and moving the location of x_2, i.e., (10-50-90%) and (10-65-90%).

Model parameters $\theta_{3,j}$		
FFOPDT (10-90%)	**FFOPDT (10-50-90%)**	**FFOPDT (10-65-90%)**
$K_{3,1} = 1.40^oC/\%$	$K_{3,2} = 1.40^oC/\%$	$K_{3,3} = 1.40^oC/\%$
$T_{3,1} = 47.17$ s	$T_{3,2} = 49.83$ s	$T_{3,3} = 46.62$ s
$L_{3,1} = 11.42$ s	$L_{3,2} = 11.08$ s	$L_{3,3} = 11.49$ s
$\alpha_{3,1} = 0.9390$	$\alpha_{3,2} = 0.9468$	$\alpha_{3,3} = 0.9373$

TABLE 13. Time-domain model performance indices $S(\theta_{3,j})$ for the experimental controlled process considering different identification methods.

j	Method	Set of points	$S(\theta_{3,j})$
1	Proposed	(10-90%)	$6.63 \cdot 10^{-5}$
2	Symmetrical	(10-50-90%)	$7.33 \cdot 10^{-5}$
3	Asymmetrical	(10-65-90%)	$7.07 \cdot 10^{-5}$
Number of samples: $N_S = 4,001$			

Table 12 presents the FFOPDT model parameters obtained for the thermal-based process at the considered operating point using the proposed identification method with set of points (10)-90%). The parameters of the FFOPDT models obtained by the identification method proposed by Gude in [38] for symmetrical and asymmetrical set of points have also been included in this table.

Next, the process reaction curve is compared with the step response of the corresponding FFOPDT model with the proposed method in Fig. 15.

This figure also show the corresponding representative points on the process reaction curve.

Table 13 shows the values of the time-domain model performance index $S(\theta_{3,j})$ for the different identification methods ($j = 1, 2, 3$) applied to the experimental thermal-based controlled process. The values of the relative model performance index $S_{3,j} = S(\theta_{3,1})/S(\theta_{3,j})$ are shown in Table 14 and graphically illustrated in Fig. 16. Although it has been shown in [36] that the symmetrical and asymmetrical methods give good resuls, this figure shows that the model obtained with the proposed method reduces by 10% and 7% the value of S with respect to the models obtained with the method proposed by Gude and García Bringas, for the symmetrical (10-50-90%) and asymmetrical (10-65-90%) set of points, respectively.

D. DISCUSSION

In this section, several examples have been used to illustrate the effectiveness and applicability of the proposed

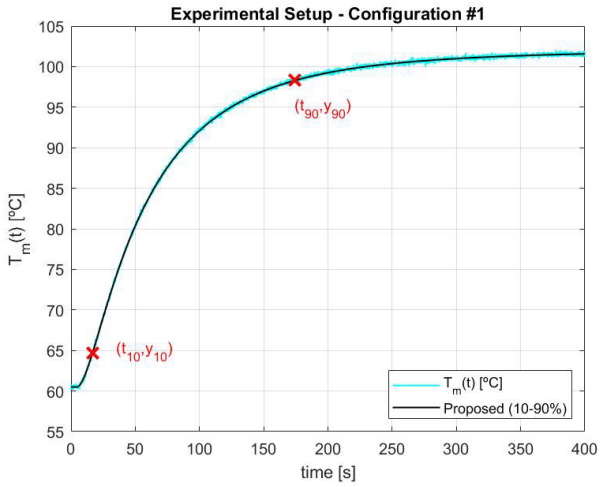

FIGURE 15. Process reaction curve $T_m(t)$ [^oC] and FFOPDT model step response using the proposed identification method for (10-90%). Representative points $x_1 = 10\%$ and $x_3 = 90\%$ on the process reaction curve are also displayed. The accuracy of the identified model is remarkable in the figure.

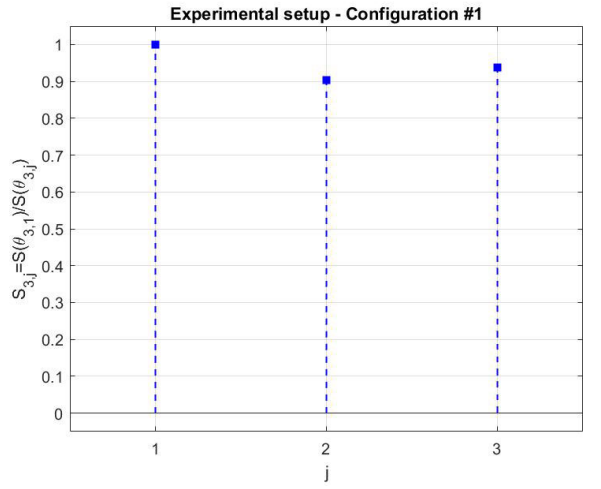

FIGURE 16. Model performance index values $S(\theta_{3,j})$ obtained with methods #1–3 for the experimental controlled process.

TABLE 14. Relative performance indexes obtained with different identification methods ($j = 1, 2, 3$) in comparison with the proposed method ($j = 1$) for thermal-based process P_3. The improvement obtained by using the proposed method is also illustrated in this table.

j	Compared methods	$S_{3,j}$	Improvement
1	Proposed-Proposed	1.0000	–
2	Proposed-Symmetrical	0.9045	10%
3	Proposed-Asymmetrical	0.9378	7%

identification method. On the one hand, the first two examples demonstrate the effectiveness of the proposed identification method compared to other methods for fractional-order models. On the other hand, the third example allows verifying the applicability of the proposed identification method by implementing the proposed identification algorithm on microprocessor-based control hardware and applying it to a thermal-based experimental setup.

The identification method proposed in this paper is compared with the following identification procedures. The potential advantages of the proposed identification method are treated below, providing a discussion on the comparison:

1) The integral-based method followed by Tavakoli-Kakhki [33] is a pioneering method in estimating FFOPDT model parameters and is used in numerous studies as a reference method for comparing new identification proposals. In this reference, three different strategies are proposed to determine the parameters of the fractional-order model. Given that the model parameters K and α obtained using the proposed method are identical to those proposed by Tavakoli-Kakhki, Examples 1 and 2 show that the superiority of the proposed method is due to a more accurate estimation of parameters T and L. In this regard, the estimation of T and L using Tavakoli-Kakhki's method is based on numerical computation of the fractional-order integral of a given function, in contrast, the one of the proposed method is analytical. Similar integral-based methods have been proposed by Tavakoli-Kakhki and co-workers in [34] and [35]. These methods are characterized by their efficiency in the presence of measurement noise. The same conclusions can be obtained with the latter methods as those obtained by comparing the proposed method with [33]. Both the method proposed in this paper and the methods proposed by Tavakoli-Kakhki describe the dynamics of processes having an S-shaped step response using the FFOPDT model with order $\alpha \leq 1.0$.
2) Gude and García Bringas proposed different FFOPDT model identification procedures based on fitting three points on the process reaction curve [36], [37], [38].
For the sake of fairness in comparison, the symmetrical and asymmetrical procedures proposed by Gude and García Bringas used for the comparison also employ $x_1 = 10\%$ and $x_3 = 90\%$ points on the reaction curve, as does the proposed method.
Note that the proposed method is general for any arbitrary values of x_1 and x_3 on the reaction curve.
In the context of FFOPDT model identification methods based on fitting three points on the process reaction curve, [37] establishes that the step response of the identified model provides a good fit with the process reaction curve, especially in the interval $[x\text{-}(100 - x)]$, with $x_1 = x$ and $x_3 = 100 - x$. Correspondingly, it can be suggested for the proposed method that a longer $[x_1 - x_3]$ interval allows the model to better fit the process reaction curve, which results in a lower value in the model performance index S.
The following conclusions can be drawn from comparative analysis of the previous methods proposed by Gude and García Bringas with the one proposed in this work:
   - The method presented in this paper is proposed within the same framework as the methods

proposed in [36], [37], and [38], providing a more accurate estimation of the FFOPDT model.
- Since model parameters T and L depend on the location of points x_1 and x_3, the model improvement obtained by the proposed method results from a more accurate estimation of α.
- Therefore, the efficiency and simplicity of implementation, which are key aspects in industry and characterize the previous methods proposed by Gude and García Bringas, are maintained in the current proposal.

3) The method proposed by Guevara et al. [31] deals with the identification of FFOPDT model parameters using an optimization-based method. The criterion applied is the minimization of the integral of the absolute error, which is the difference between the model step response and the process reaction curve. This method is applicable to processes with overdamped or underdamped step responses, i.e., characterized with a fractional order $0.0 \leq \alpha \leq 2.0$ that can be estimated from the process reaction curve.
   Regarding the comparison of this method with the proposed method, Example 1 shows that the analytical methods (proposed, symmetrical, and asymmetrical) can provide results as good as or even better than those obtained by the optimization-based methods. Optimization-based methods are generally more complicated and require a higher computational effort than analytical methods.
   Note also that the approximation of the fractional part of the model is performed in Guevara's method by applying the CRONE approach, see [55], while the Grünwald-Letnikov definition is used in the proposed method for numerical computation of fractional-order derivatives.
4) Numerous methods for identifying integer-order models have been presented in the introduction. However, only the optimal FOPDT model has been used in the illustrative examples in Section IV. Note that the cost function used to obtain the optimal model is (32), therefore, the FOPDT model obtained will be the one with a lower S value.
   Moreover, the superiority of fractional-order models over integer-order ones to identify processes with fractional behavior is well-known in the technical literature, see, e.g., [36], [37], and [39]. This can also be verified in Example 1.

V. FUTURE WORKS

In the context of the work presented in this paper, the following can be included as research lines and future work:

- The identification method proposed in this work is restricted to fractional order values in the range $0.5 \leq \alpha \leq 1.0$, and as future work we propose to develop this identification method using the same methodology for processes with underdamped step response, extending the fractional order range to $1.0 \leq \alpha \leq 2.0$.
- In this work, microprocessor-based hardware has been used for the implementation of the proposed fractional-order identification algorithm, which has verified its applicability in an industrial environment. As future work, it is proposed to implement this identification procedure in hardware devices such as PLCs, which are undoubtedly the workhorse of the process industry.

VI. CONCLUSION

This paper presented a new FFOPDT model identification method to characterize the dynamic response of a system with an S-shaped step response.

The results of the examples used in this work show this procedure's effectiveness in identifying fractional-order models. The applicability of the proposed analytical procedure and the simplicity of implementation on industrial hardware and applied to a thermal-based laboratory prototype is also shown.

We believe that this type of identification procedure, in which simplicity is the main feature, will encourage the adoption of fractional-order models and their practical application in the process industry.

REFERENCES

[1] G. F. Franklin, J. D. Powell, and A. Emami-Naeini, *Feedback Control of Dynamic Systems*. London, U.K.: Pearson, 2019.
[2] K. J. Åström and T. Hägglund, *Advanced PID Control*, vol. 461. Research Triangle Park, NC, USA: ISA-The Instrumentation, Systems, and Automation Society, 2006.
[3] R. Vilanova and A. Visioli, *PID Control in the Third Millennium*. Cham, Switzerland: Springer, 2012.
[4] O. Garpinger, T. Hägglund, and K. J. Åström, "Performance and robustness trade-offs in PID control," *J. Process Control*, vol. 24, no. 5, pp. 568–577, May 2014.
[5] T. Liu and F. Gao, *Industrial Process Identification and Control Design: Step-Test and Relay-Experiment-Based Methods*. Berlin, Germany: Springer, 2011.
[6] J. Crowe, K. Tan, T. Lee, R. Ferdous, M. Katebi, H.-P. Huang, J.-C. Jeng, K. Tang, G. Chen, and K. Man, "Process reaction curve and relay methods identification and PID tuning," in *PID Control: New Identification and Design Methods*. London, U.K.: Springer, 2005, pp. 297–337, doi: 10.1007/1-84628-148-2.
[7] L. Ljung, "Identification for control: Simple process models," in *Proc. 41st IEEE Conf. Decis. Control*, Jul. 2002, pp. 4652–4657.
[8] K. K. Tan, Q.-G. Wang, and C. C. Hang, *Advances in PID Control*. Berlin, Germany: Springer, 2012.
[9] G. P. Rangaiah and P. R. Krishnaswamy, "Estimating second-order dead time parameters from underdamped process transients," *Chem. Eng. Sci.*, vol. 51, no. 7, pp. 1149–1155, 1996, doi: 10.1016/S0009-2509(96)80013-3.
[10] H.-P. Huang, M.-W. Lee, and C.-L. Chen, "A system of procedures for identification of simple models using transient step response," *Ind. Eng. Chem. Res.*, vol. 40, no. 8, pp. 1903–1915, Apr. 2001.
[11] V. Alfaro, "Low-order models identification from the process reaction curve," *Ciencia y Tecnología (Costa Rica)*, vol. 24, no. 2, pp. 197–216, 2006.
[12] W. K. Ho, C. C. Hang, and L. S. Cao, "Tuning of PID controllers based on gain and phase margin specifications," *Automatica*, vol. 31, no. 3, pp. 497–502, Mar. 1995.
[13] C. L. Smith, *Digital Computer Process Control*. Scranton, PA, USA: Intext Educational Publishers, 1972.

[14] V. Miluše, A. Víteček, and L. Smutný, "Simple PI and PID controllers tuning for monotone self-regulating plants," *IFAC Proc. Volumes*, vol. 33, no. 4, pp. 259–264, Apr. 2000.
[15] A. Jahanmiri and H. R. Fallahi, "New methods for process identification and design of feedback controller," *Chem. Eng. Res. Design*, vol. 75, no. 5, pp. 519–522, Jul. 1997.
[16] R. A. Mollenkamp, *Introduction to Automatic Process Control*. Research Triangle Park, NC, USA: ISA International Society for Measurement and Control, 1984.
[17] G. P. Rangaiah and P. R. Krishnaswamy, "Estimating second-order plus dead time model parameters," *Ind. Eng. Chem. Res.*, vol. 33, no. 7, pp. 1867–1871, Jul. 1994.
[18] G. Sales Teodoro, J. A. Tenreiro Machado, and E. Capelas de Oliveira, "A review of definitions of fractional derivatives and other operators," *J. Comput. Phys.*, vol. 388, pp. 195–208, Jul. 2019.
[19] C. Ionescu, A. Lopes, D. Copot, J. A. T. Machado, and J. H. T. Bates, "The role of fractional calculus in modeling biological phenomena: A review," *Commun. Nonlinear Sci. Numer. Simul.*, vol. 51, pp. 141–159, Oct. 2017.
[20] J.-D. Gabano, T. Poinot, and H. Kanoun, "Identification of a thermal system using continuous linear parameter-varying fractional modelling," *IET Control Theory Appl.*, vol. 5, no. 7, pp. 889–899, May 2011.
[21] K. M. Owolabi and D. Baleanu, "Emergent patterns in diffusive turing-like systems with fractional-order operator," *Neural Comput. Appl.*, vol. 33, no. 19, pp. 12703–12720, Oct. 2021.
[22] K. M. Owolabi and E. Pindza, "Numerical simulation of chaotic maps with the new generalized caputo-type fractional-order operator," *Results Phys.*, vol. 38, Jul. 2022, Art. no. 105563.
[23] A. Tepljakov, B. B. Alagoz, C. Yeroglu, E. Gonzalez, S. H. HosseinNia, and E. Petlenkov, "FOPID controllers and their industrial applications: A survey of recent results," *IFAC-PapersOnLine*, vol. 51, no. 4, pp. 25–30, 2018.
[24] I. Birs, C. Muresan, I. Nascu, and C. Ionescu, "A survey of recent advances in fractional order control for time delay systems," *IEEE Access*, vol. 7, pp. 30951–30965, 2019.
[25] A. A. Dastjerdi, B. M. Vinagre, Y. Chen, and S. H. HosseinNia, "Linear fractional order controllers; a survey in the frequency domain," *Annu. Rev. Control*, vol. 47, pp. 51–70, Jun. 2019.
[26] P. Shah and S. Agashe, "Review of fractional PID controller," *Mechatronics*, vol. 38, pp. 29–41, Sep. 2016.
[27] C. A. Monje, Y. Chen, B. M. Vinagre, D. Xue, and V. Feliu-Batlle, *Fractional-Order Systems and Controls: Fundamentals and Applications*. Berlin, Germany: Springer, 2010.
[28] A. Tepljakov, *Fractional-Order Modeling and Control of Dynamic Systems*. Cham, Switzerland: Springer, 2017.
[29] H. Malek, Y. Luo, and Y. Chen, "Identification and tuning fractional order proportional integral controllers for time delayed systems with a fractional pole," *Mechatronics*, vol. 23, no. 7, pp. 746–754, Oct. 2013.
[30] S. Ahmed, "Parameter and delay estimation of fractional order models from step response," *IFAC-PapersOnLine*, vol. 48, no. 8, pp. 942–947, 2015.
[31] E. Guevara, H. Meneses, O. Arrieta, R. Vilanova, A. Visioli, and F. Padula, "Fractional order model identification: Computational optimization," in *Proc. IEEE 20th Conf. Emerg. Technol. Factory Autom. (ETFA)*, Sep. 2015, pp. 1–4.
[32] B. B. Alagoz, A. Tepljakov, A. Ates, E. Petlenkov, and C. Yeroglu, "Time-domain identification of one noninteger order plus time delay models from step response measurements," *Int. J. Model., Simul., Sci. Comput.*, vol. 10, no. 1, Feb. 2019, Art. no. 1941011.
[33] M. Tavakoli-Kakhki, M. Haeri, and M. Saleh Tavazoei, "Simple fractional order model structures and their applications in control system design," *Eur. J. Control*, vol. 16, no. 6, pp. 680–694, Jan. 2010.
[34] M. Tavakoli-Kakhki, M. S. Tavazoei, and A. Mesbahi, "Parameter and order estimation from noisy step response data," *IFAC Proc. Volumes*, vol. 46, no. 1, pp. 492–497, Feb. 2013.
[35] M. Tavakoli-Kakhki and M. S. Tavazoei, "Estimation of the order and parameters of a fractional order model from a noisy step response Data," *J. Dyn. Syst., Meas., Control*, vol. 136, no. 3, May 2014, Art. no. 031020.
[36] J. J. Gude and P. García Bringas, "Proposal of a general identification method for fractional-order processes based on the process reaction curve," *Fractal Fractional*, vol. 6, no. 9, p. 526, Sep. 2022.
[37] J. J. Gude and P. García Bringas, "Influence of the selection of reaction curve's representative points on the accuracy of the identified fractional-order model," *J. Math.*, vol. 2022, pp. 1–22, Jun. 2022.
[38] J. J. Gude, "Contributions to fractional-order modelling and control of dynamic systems: A theoretical and practical approach," Ph.D. dissertation, Univ. Deusto, Bilbao, Spain, 2023.
[39] J. J. Gude and P. García Bringas, "A novel control hardware architecture for implementation of fractional-order identification and control algorithms applied to a temperature prototype," *Mathematics*, vol. 11, no. 1, p. 143, Dec. 2022.
[40] J. Sabatier, C. Farges, and V. Tartaglione, *Fractional Behaviours Modelling: Analysis and Application of Several Unusual Tools*, vol. 101. Berlin, Germany: Springer Nature, 2022.
[41] I. Podlubny, *Fractional Differential Equations, Mathematics in Science and Engineering*. New York, NY, USA: Academic press, 1999.
[42] S. Das, *Functional Fractional Calculus*, vol. 1. Cham, Switzerland: Springer, 2011.
[43] K. M. Owolabi and A. Atangana, *Numerical Methods for Fractional Differentiation*. Cham, Switzerland: Springer, 2019, vol. 54.
[44] A. A. Kilbas, H. M. Srivastava, and J. J. Trujillo, *Theory and Applications of Fractional Differential Equations*, vol. 204. Amsterdam, The Netherlands: Elsevier, 2006.
[45] K. S. Miller and B. Ross, *An Introduction to the Fractional Calculus and Fractional Differential Equations*. Hoboken, NJ, USA: Wiley, 1993.
[46] A. A. Kilbas, O. Marichev, and S. Samko, *Fractional Integrals and Derivatives* (Theory and Applications). Philadelphia, PA, USA: Gordon & Breach, 1993.
[47] J. Ceballos, N. Coloma, A. Di Teodoro, D. Ochoa-Tocachi, and F. Ponce, "Fractional multicomplex polynomials," *Complex Anal. Operator Theory*, vol. 16, no. 4, pp. 1–30, Jun. 2022.
[48] N. Coloma, A. Di Teodoro, D. Ochoa-Tocachi, and F. Ponce, "Fractional elementary bicomplex functions in the Riemann–Liouville sense," *Adv. Appl. Clifford Algebras*, vol. 31, no. 4, p. 63, Sep. 2021.
[49] I. Podlubny, "Fractional-order systems and fractional-order controllers," *Inst. Experim. Phys., Slovak Acad. Sci., Kosice*, vol. 12, no. 3, pp. 1–18, 1994.
[50] J. Ceballos, N. Coloma, A. D. Teodoro, and D. Ochoa-Tocachi, "Generalized fractional Cauchy–Riemann operator associated with the fractional Cauchy–Riemann operator," *Adv. Appl. Clifford Algebras*, vol. 30, no. 5, pp. 1–22, Nov. 2020.
[51] R. Gorenflo, A. A. Kilbas, F. Mainardi, and S. V. Rogosin, *Mittag-Leffler Functions, Related Topics and Applications*. Cham, Switzerland: Springer, 2020.
[52] S. Rogosin, "The role of the Mittag-Leffler function in fractional modeling," *Mathematics*, vol. 3, no. 2, pp. 368–381, May 2015.
[53] D. Xue, *Fractional-Order Control Systems*. Berlin, Germany: de Gruyter, 2017.
[54] J. J. Gude and P. García Bringas, "Proposal of a control hardware architecture for implementation of fractional-order controllers," in *Proc. 16th Int. Conf. Dyn. Syst. Theory Appl. (DSTA)*, Lodz, Poland, 2021, pp. 6–9.
[55] A. Oustaloup, J. Sabatier, P. Lanusse, R. Malti, P. Melchior, X. Moreau, and M. Moze, "An overview of the CRONE approach in system analysis, modeling and identification, observation and control," *IFAC Proc. Volumes*, vol. 41, no. 2, pp. 14254–14265, 2008.

JUAN J. GUDE received the bachelor's degree in applied physics from the Faculty of Science, University of the Basque Country (UPV/EHU), Leioa, Spain, and the Ph.D. degree from the University of Deusto, Bilbao, Spain. The research topic of his thesis was fractional-order modeling and control of dynamical systems. He has been with the Department of Computing, Electronics and Communication Technologies, University of Deusto, since 2001. He is currently a Senior Lecturer and has been responsible for the Laboratory of Measuring Systems and Control, Faculty of Engineering, University of Deusto, during the last 20 years. He has extensive experience in the development of innovative industrial prototypes for the theoretical and practical training of engineers in process control, industrial automation, and industrial communications. In this regard, he has participated in the construction and commissioning of numerous prototypes for various institutions. His teaching and research activities have been related to applied industrial control, control systems, and industrial systems and equipment. His research interests include modeling, analysis, and control of dynamic systems in particular fractional-order systems.

ANTONIO DI TEODORO received the Ph.D. degree from Universidad Simón Bolívar (USB), Caracas, Venezuela, in 2010. He has had the opportunity to lead, teach, and investigate mathematics with USB; Yachay Tech University, Ecuador; Penn State University, USA; and Universidad San Francisco de Quito (USFQ), Ecuador. He is currently a Professor and the Head of the Department of Mathematics, USFQ. He is a mathematician on fractional calculus in hypercomplex analysis.

OSCAR CAMACHO (Senior Member, IEEE) received the bachelor's degree in electrical engineering and the M.Sc. degree in control engineering from Universidad de Los Andes (ULA), Mérida, Venezuela, in 1984 and 1992, respectively, and the M.E. and Ph.D. degrees in chemical engineering from the University of South Florida (USF), USA, in 1994 and 1996, respectively. He was a Postdoctoral Researcher in development activities with USF, in 2001. He was the Head of the School of Electrical Engineering, a Coordinator with the Master's Program in Automation and Instrumentation, and the Dean of the Faculty of Engineering, ULA, from 2005 to 2014. He has held teaching and research positions with ULA; PDVSA, Venezuela; USF; Escuela Politécnica Nacional, Ecuador. He is currently with Universidad San Francisco de Quito (USFQ), Quito, Ecuador. He has published more than 200 publications in journals and conference proceedings. His current research interests include sliding mode control and long delay process control systems. He is an Associate Editor of *ISA Transactions*.

PABLO GARCÍA BRINGAS received the engineering degree in computer science, the master's degree in telecommunications, the master's degree in industrial informatics, the Ph.D. degree in computer science and artificial intelligence (specialized on cyber-security), and the Executive Master's degree in business administration. He is currently an University Associate Professor (Profesor Titular de Universidad) and the Vice Dean of External Affairs. He is also the Head Researcher of the Deusto for Knowledge-D4K Research Group. Previously, he has been the Director of the DeustoTech-Deusto Institute of Technology, the Director of Research of the Faculty of Engineering, and the Director of the Deusto's Chair on Digital Industry. He has more than 20 years of experience in research and development management, with tens of projects and technology transfer actions led, for more than ten million euro, more than 40 ISI-JCR impact factor publications, more than 120 international peer-reviewed contributions, and 19 Ph.D. supervised dissertations. His research interests include artificial intelligence applied to the fields of information security and industrial processes. He has co-chaired world-class scientific events, such as DEXA, CISIS, SOCO, ICEUTE, HAIS, INFOSEC, and BIGDAT or DEEP LEARNING BILBAO!.